

Optimizing the High-Pass Filter Addition Technique for Image Fusion

Ute G. Gangkofner, Pushkar S. Pradhan, and Derrold W. Holcomb

Abstract

Pixel-level image fusion combines complementary image data, most commonly low spectral-high spatial resolution data with high spectral-low spatial resolution optical data. The presented study aims at refining and improving the High-Pass Filter Additive (HPFA) fusion method towards a tunable and versatile, yet standardized image fusion tool. HPFA is an image fusion method in the spatial domain, which inserts structural and textural details of the higher resolution image into the lower resolution image, whose spectral properties are thereby largely retained. Using various input image pairs, workable sets of HPFA parameters have been derived with regard to high-pass filter properties and injection weights. Improvements are the standardization of the HPFA parameters over a wide range of image resolution ratios and the controlled trade-off between resulting image sharpness and spectral properties. The results are evaluated visually and by spectral and spatial metrics in comparison with wavelet-based image fusion results as a benchmark.

Introduction

Pixel-based image fusion techniques amalgamate the physical properties of the source images into a new image. The most frequent application for image fusion is what many authors call resolution merging or pan-sharpening, where multispectral data of coarser spatial resolution are merged with data of finer spatial resolution, usually panchromatic (PAN) imagery. The result is an artificial multispectral image with the spatial resolution of the panchromatic image (Steinnocher 1999). The perfect pan-sharpening result would be identical to the image the multispectral sensor would have observed if it had the spatial resolution of the panchromatic sensor (Wald *et al.*, 1997). That means the goal of pan-sharpening is to render a sharpened image incorporating the full spatial information content of the panchromatic image without introducing spectral distortions to the multispectral input data. Not only is spectral fidelity of the fusion result important for visual image interpretation, it is also essential for automatic image classification approaches (Pradhan *et al.*, 2006).

Several currently operating optical sensors (e.g., SPOT, Landsat, QuickBird, Ikonos, etc.) generate such a combination of higher resolution panchromatic and lower resolution multispectral data. Because they are limited by the data transmission rates, the multispectral bands are recorded in a lower resolution and only the panchromatic band is transmitted at its full resolution (Pradhan, 2005). In addition, pan-sharpening can also be applied to images from different sensors, which widens the scope (i.e., ground resolution ratios, R) and consequently the methodological requirements for such image fusions. Within multi-sensor image fusion of complementary sensors, a focus can be observed on the fusion of radar data and optical data. Radar/optical image fusion can be used for image enhancement purposes (Garzelli, 2002) as well as to “fill in” missing image parts obscured by clouds in optical data (Arellano, 2003), or as a sort of resolution merge (Mercer *et al.*, 2005).

Short Overview of Existing Image Fusion Approaches

Image fusion procedures are often subdivided according to the abstraction level of the fusion, where pixel-based, feature-based, and decision-based approaches are distinguished (Pohl and Van Genderen, 1998). Within pixel-based image fusion, a rough distinction can be made between the commonly applied spectral substitution techniques (Intensity-Hue-Saturation (IHS), Principal Components (PC)), arithmetic merging (e.g., multiplicative merging, Brovey transform), and methods in the spatial domain (e.g., wavelet, HPFA).

Spectral substitution techniques have been widely discussed in the literature with varying, partly contradictory, results. Lemeshefsky (2002) discusses some theoretical limitations of IHS sharpening and suggests that sharpening of the bands individually may be preferable. Yocky (1995) demonstrates that the IHS transform can distort colors (particularly red) and discusses theoretical explanations. Nunez *et al.* (1999) compare three IHS calculations and settle for the intensity on $I = (R + G + B)/3$ as the most appropriate. While the IHS method is limited to three input bands, the PC method will accept any number of input data layers. Lemeshefsky (2002) suggested that this technique produces an output image that better preserves the numerical integrity of the input dataset than the IHS method. Zhang (1999), however, has reached the opposite conclusion regarding the PC versus IHS approaches.

Among arithmetic merging methods, a variety of approaches exist involving different arithmetic operations

U.G. Gangkofner is with GeoVille Information Systems GmbH, Museumstr. 9–11, A - 6020 Innsbruck, Austria (gangkofner@geoville.com).

P.S. Pradhan is with Photodynamics Inc. 5970 Optical Court, San Jose, CA, and formerly with the Department of Electrical and Computer Engineering, Mississippi State University, Mississippi State, MS 39759.

D.W. Holcomb is with Leica Geosystems, Atlanta, GA 30329.

Photogrammetric Engineering & Remote Sensing
Vol. 74, No. 9, September 2008, pp. 1107–1118.

0099-1112/08/7409-1107/\$3.00/0
© 2008 American Society for Photogrammetry
and Remote Sensing

(Zhang, 1999), but most of these have significant shortcomings. For example, the Brovey transform is limited to three bands and the multiplicative techniques introduce significant radiometric distortion. In addition, successful application of these techniques requires an experienced analyst (Zhang, 2002) for the specific adaptation of parameters. This precludes development of a user-friendly automated tool.

Many authors have found fusion methods in the spatial domain (high frequency inserting procedures) superior over the other approaches, which are known to deliver fusion results that are spectrally distorted to some degree (Wald *et al.*, 1997; Aiazzi *et al.*, 2003; Ehlers, 2005). Within the spatial domain techniques, the wavelet-based image fusion technique, with its large number of sub-varieties, has been most intensely investigated (e.g., Pradhan, 2005; Pradhan *et al.*, 2006; Aiazzi *et al.*, 2002; King *et al.*, 2001). The far less complex HPFA method, which basically consists of addition of the PAN-derived HP information to the multispectral bands, received comparatively little attention and was partly rejected as inferior (e.g., Aiazzi *et al.*, 2003).

Zhang (2002) summarizes the essential problems of available image fusion techniques as being the color distortion and dependency of the fusion quality on the operator and input data used. The author developed a new fusion method based on least squares for a best approximation of the grey value relationship between the original multispectral, panchromatic, and the fused image bands for an optimal color representation.

Objective

This paper describes a methodology, parameters, and test results for image fusion based on the High-Pass Filter Additive (HPFA) technique. The objective is a refinement of this method by means of an adaptation and standardization of its parameters to make it easily applicable to a wide range of image pairs with satisfying and tunable results. The algorithm was implemented using the ERDAS Imagine® Modeler and tested using a broad range of image pairs of varying resolution ratios (R) from multiple sensors. The test images included panchromatic and multispectral images from a common platform (Landsat, QuickBird) as well as (partly synthesized) panchromatic images and multispectral images from different platforms, including aerial photography. Finally, the developed HPFA tool is test-applied to a radar/multispectral image pair for demonstration purposes.

The HPFA Fusion Method

The HPFA technique was first introduced by Schowengerdt (1980) for reducing data volume and increasing the spatial resolution of Landsat MSS data (Carter, 1998). Chavez *et al.* (1991) extended this approach to more diverse multi-resolution data sets and found that resolution merging using the HPFA technique preserves the spectral content of the original multispectral data better than the IHS or PCA techniques. The HPFA technique has generally been implemented in a simplistic way. Its parameters have, to the knowledge of the authors, not been optimized to deliver satisfying spatial and spectral results for a broad spectrum of multi-resolution and multi-sensor data merges.

Previous Findings with Regard to HPFA Parameters

The HPFA fusion method in its original implementation is only minimally described in the literature and is very straightforward. The basic idea is analogous to the more complex methods of this family, such as wavelet (see the next section) and Laplacian pyramid (Aiazzi *et al.*, 2003). High frequency information (derived with a high-pass filter from a panchromatic, SAR, or other spatially detailed image)

is incorporated, in this case using addition, into the lower resolution multispectral image. As opposed to those more complex methods such as wavelet-based image fusion, the HPFA method uses standard, square box HP filters. As an example, a 5*5 pixel kernel is shown following:

$$\begin{matrix} -1 & -1 & -1 & -1 & -1 \\ -1 & -1 & -1 & -1 & -1 \\ -1 & -1 & 24 & -1 & -1 \\ -1 & -1 & -1 & -1 & -1 \\ -1 & -1 & -1 & -1 & -1 \end{matrix}$$

In its simplest form, the HP filter matrix is occupied by “-1” at all but the center location. The center value is derived by $c = n*n - 1$, where c is the center value and $n*n$ is the size of the filter box. Thus, a 7 by 7 HP filter has a center value of 48, and a 9 by 9 HP filter has a center value of 80.

The HP filtering of the PAN image extracts the spatial details, analogous to the use of the wavelet transform in wavelet-based fusion (see the *Wavelet Transform and Wavelet-based Image Fusion* section). However, only one application of a HP filter and, consequently, one intermediate image file is needed to derive and store the detail information of a certain image frequency.

For resolution merging, an optimal kernel size for the HPF was found to be about twice the resolution ratio of the images (Chavez *et al.*, 1991). For Landsat ETM+ resolution merges, the resolution ratio is 2 because we are dealing with 30 m multispectral and 15 m panchromatic images. In this case, the PAN image would be filtered with a 5*5 pixel HP filter, corresponding to 2.5*2.5 multispectral pixels.

As an injection model for incorporating the HPF detail into the lower resolution multispectral image, it has been reported to add the HP filtered image to each multispectral band and then divide each result by two to offset the increase in brightness values (Carter, 1998). However, fairly strong contrast enhancement may be needed afterwards to get visually satisfying results.

In this study, variations in both the kernel matrix size and the center value are evaluated and optimized. In addition, a more sophisticated injection model, though still involving an addition of the HP details and the multispectral bands, is found to routinely produce satisfying results.

Aiazzi *et al.* (2003) point out that “the poor performance of the HPFA technique is due to the box filter having little frequency selection, as well as to the absence of an injection model.” In this study, the lack of frequency selection was found to be unsatisfactory only for pan-sharpening image pairs with resolution ratios greater than 5. A solution for these cases is proposed below. The lack of an injection model, in addition to being responsible for the often inferior results of the HPFA method, also prevents its use as a standard image fusion tool with broad applicability.

The HPFA Technique as Developed in this Study

The HPFA technique has been optimized using a wide variety of test images. The HP filter and the injection parameters were initially determined by visually assessing and comparing the fusion results. For reference and fine tuning, several wavelet-based fusion results and spectral/spatial fusion quality metrics were used (see the Analysis section). The HPFA technique as developed in this research is comprised of the following steps (see Figure 1 for an overview):

Step 1: HP Filtering of the High-resolution Image to Extract the Structural Detail

Previous findings with respect to the kernel size, largely confirmed in this study, indicate that an adequate kernel

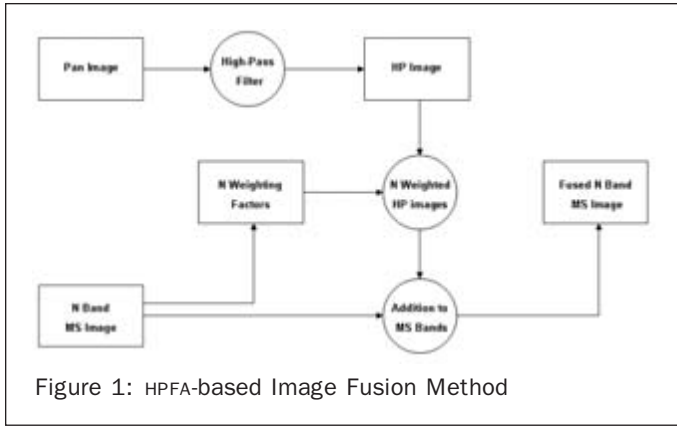


Figure 1: HPFA-based Image Fusion Method

size is approximately twice the resolution ratio (actually, $2R + 1$) of the image pairs when dealing with resolution ratios of 2 to 5. For larger ratios the kernel size, as determined by empirical testing, becomes smaller in relation to the resolution ratio; it was capped at a size of 15×15 in this study. The largest resolution ratio tested was 10: fusion of a degraded aerial photograph (3 m) with a (30 m) multispectral Landsat image (30 m) and fusion of ASAR (30 m) with simulated MERIS (300 m) data.

In addition to kernel size, the kernel center value was varied in this study. As described above, the standard HP filter center value is given by $n \times n - 1$, where $n \times n$ is the size of the filter kernel. An increase in the center value (i.e., a higher weighting of the center pixel during the convolution) means that the radiometric response of panchromatic image is more intensely incorporated into the filtered image and, consequently, into the fusion result. In some cases, the increased center values improve the visual properties (but not the spectral fidelity) of the fusion results by reducing false edges. The latter are introduced by contrast reversal as a result of different band passes for the panchromatic and the multispectral bands. However, increasing the center value of the HP filter matrix will lead to a decrease in color saturation and possibly to an increase in the overall contrast of the fused images. A decrease of the center value of the HPF kernel, on the other hand, leads to an increase in the color saturation of the fused image with, however, possible impairment of edges. Nevertheless, applied with care (i.e., suitable injection weights, see below), a slight decrease (10 to 20 percent) in the center value may help to create superior fusion results with minimal loss of color saturation. This is especially true for small objects (Plate 1c, 1d, 1e, and 1f).

For resolution merges of intermediate resolution ratios (5 to 6) and larger ratios (>6), it was found that the PAN sharpening could be further improved by adding a second HP filtered image, derived with a small filter kernel, to the fused image. This second injection brought a further enhancement of small area structural and textural details, because it compensates for the lack of very high frequency information as the filter kernel gets larger. The most appropriate filter kernel size for this second kernel was empirically determined to be 5×5 pixels for all resolution ratios, regardless of the dimension of the primary kernel. This procedure is hereafter referred to as “Two-Pass” (see Plate 1a and 1b). The combined weighting given to the two HPF images in the “Two-Pass” result is the same as the weight given to the HPF image of the “One-Pass” technique.

Step 2: Adding the HP Filtered Image to Each Band of the Multispectral Image Using a Standard Deviation-based Injection Model

In the next step, the HP filtered image is added to each multispectral (MS) band. Here the injection weight for the added HPF image is the critical parameter. This must be determined using an injection model in order to standardize the method. It was found that the ideal weight varies with the resolution ratio, the HPF kernel size and center value, the preferences of the analyst, and the application of the fused image. A fundamental finding of this study is that the injection weight can be derived as a percentage of the global standard deviation (SD) of each individual multispectral band. It was found to range from 20 percent to 25 percent ($R = 2$) of the SD to 150 percent and more ($R = 10$). However, it was concluded that for all MS bands of an image the same relative weight of the HP filtered image can be used. This internal consistency suggests that this is a robust injection model. Plate 2a shows two pan-sharpened versions of a QuickBird image, where the injection weight was varied to produce a medium and a very crisp fusion result.

Step 3: Linear Histogram Match to Adapt SD and Mean of the Merged Image Bands to Those of the Original MS Image Bands

The last step (optional) is a linear histogram match to adapt the Standard Deviations (SD) and Means of the fused bands to those of the corresponding original MS bands. This allows for direct visual comparison of the fused image and the original MS image using the same look-up table and for evaluating the spectral fidelity of the result with quantitative metrics. A linear histogram match is sufficient, as the spectral characteristics of the image after fusion have not significantly changed. SD and Mean adaptation are, in addition, a useful means of obtaining images of the same bit format (e.g., 8-bit) as the original MS image. A disadvantage of the SD and Mean adaptation may be that the quantitative increase of structural and textural information content in the merged bands, which is reflected by an increased SD, is not retained. However, visual sharpening was not observed to decrease through histogram matching. Histogram matching does increase total computation time.

Analysis

Data

A wide variety of imagery of varying resolution ratios (2 to 10) was empirically evaluated in the initial stages of this study. The fine tuning of the HPFA fusion method was based on comparisons with wavelet-based image fusion results, using both quantitative image metrics and visual interpretation. These metrics are introduced in the following section. The three test images used for the metrics based comparison are listed in Table 1. As the available wavelet-based fusion images had only three bands (though the method is not restricted to three MS bands), the metrics for comparison were only applied to those.

The following subsection briefly describes the wavelet transform, which is the basis of wavelet-based image fusion.

Wavelet Transform and Wavelet-based Image Fusion

Wavelets are small waves that have their energy concentrated in time, which allows them to represent time or feature varying phenomena efficiently (Burrus, 1998). While the Fourier series expansion provides only a frequency analysis of a signal, the wavelet expansion provides a time-frequency analysis of the signal. That means it not only determines the frequency of a feature, but also its location.



(a)

(b)



(c)



(d)



(e)



(f)



(g)

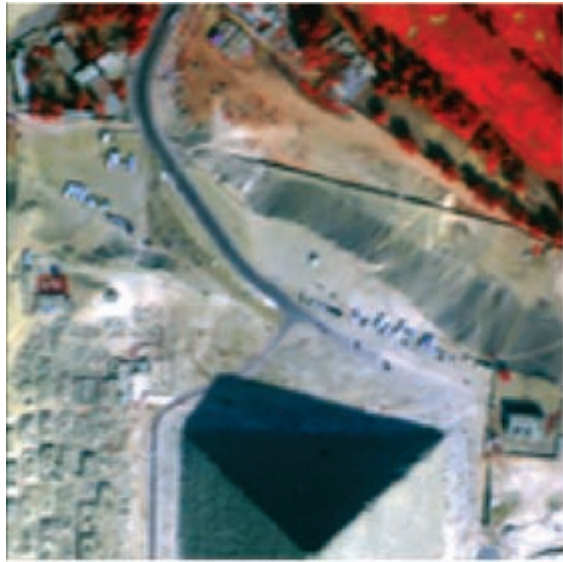


(h)



(i)

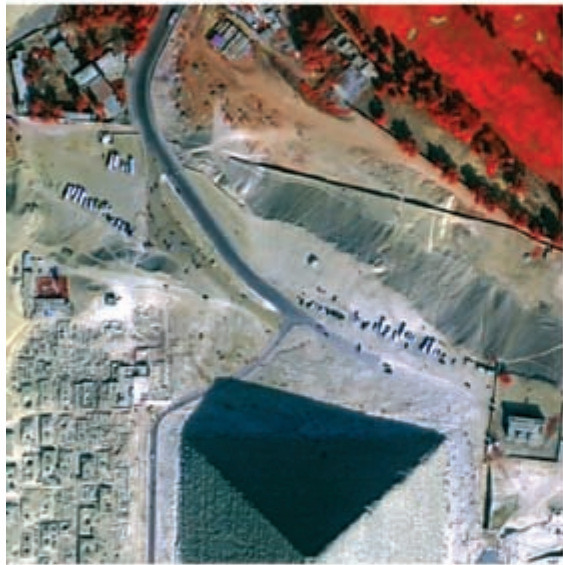
Plate 1. (a) One Pass HPFA Fusion Result, (b) Two Pass HPFA Fusion Result, (c) Original, Full Resolution Image, (d) Two Pass HPFA Fusion Result: HP 11*11: Center value 108; HP 5*5: Center value 22, (e) Two Pass HPFA Fusion Result: HP 11*11: Center value 120; HP 5*5: Center value 24, (f) Two Pass HPFA Fusion Result: HP 11*11: Center value 150; HP 5*5: Center value 28, (g) Original Airphoto, (h) HPFA Fusion Result, and (i) Wavelet-based Fusion Result.



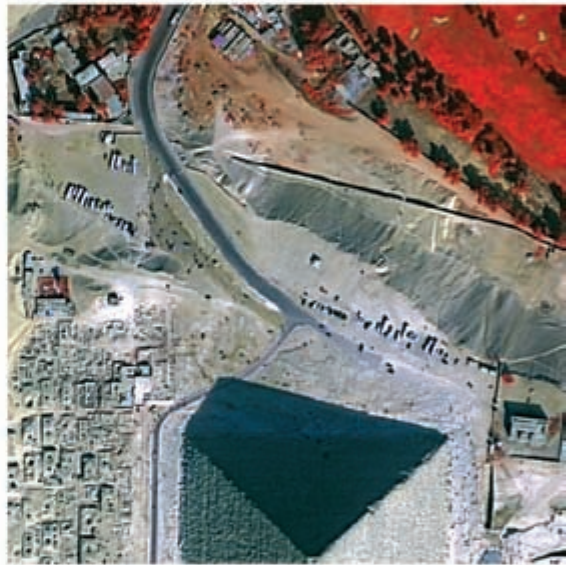
(a)



(b)



(c)



(d)



(e)



(f)



(g)

Plate 2. (a) Original QuickBird ms Image (© DigitalGlobe), Bands 4,3,1, (b) Detail: Medium – Very Crisp, (c) HPFA Fusion Result (1), Medium, (d) HPFA Fusion Result (2), Very Crisp, (e) Landsat TM Bands 1,2,3, (f) Radar Fusion Result, and (g) Radar Image (© Radarsat).

TABLE 1. TEST IMAGE SOURCES, LOCATION AND RESOLUTION RATIO

Test case No.	Image pairs and ground resolution [m]	Geographical Location	Resolution ratio (R)
1	Landsat PAN [15], Landsat MS [30]	Denver, Colorado	2
2	Landsat PAN [15], Landsat MS [30]	Vorarlberg, Austria	2
3	Aerial photography and degraded image	MSU Campus, Mississippi	4

In practical applications, filter kernels are derived to approximate the effect of the wavelets. Mallat (1989) described a filter bank implementation to compute a Discrete Wavelet Transform (DWT) (Castleman, 1996; Strang and Nguyen, 1996), where a set of low-pass and high-pass filters obtained from the wavelet basis function are convolved with the image, and the outputs of the filters are downsampled. The output low-pass and high-pass filtered images correspond to the low-frequency and high-frequency components of the image, respectively. This procedure can be recursively applied to the output of the low-pass filter, while the outputs of the high-pass filters of each iteration level are retained. The DWT of an image produces four output images (King and Wang, 2001):

1. Approximation coefficients (A): the low-pass image,
2. Horizontal coefficients (H): details along the columns,
3. Vertical coefficients (V): details along the rows, and
4. Diagonal coefficients (D): details along the diagonals.

To compensate for the fourfold increase in data volume, the DWT downsamples each coefficient image by a factor of two. However, this results in a loss of information and the transform is termed shift variant. The shift variance of the transform can sometimes be a problem in image fusion as it leads to artifacts in the fused or pan-sharpened images (González-Audicana *et al.*, 2004). It can be overcome by eliminating the sub-sampling step in the DWT, a procedure known as the Shift Invariant Discrete Wavelet Transform (SIDWT). Thus many authors, including this study, use the SIDWT because of its shift invariant properties, which avoid artifacts in the fused image.

Wavelet-based image fusion methods use the same principle as the HPFA technique, i.e., extract the high frequency (detail) information from the PAN image for insertion into the MS image. This technique is demonstrated in Figure 2. The wavelet transform (SIDWT) is applied on both the PAN and each MS band to be merged, thus separating them into their low- and high-frequency components: A, H, V, and D. The subscripts M and P are used to denote the wavelet transform images of the MS and the PAN images,

respectively. Since we want to incorporate the details from the PAN image into the MS imagery, the detail coefficients from the MS band and the approximation image of the PAN image are discarded. The detail images of the PAN (H_P, V_P, D_P) are combined with the low frequency component (A_M) of the MS imagery, using the inverse wavelet transform, to obtain the pan-sharpened MS band.

The Metrics Used for Comparing HPFA and Wavelet-based Fusion Results

This section describes the spectral and spatial quality metrics applied to assess and compare the quality of the fused images. The metrics used are a partly modified subset of the metrics presented and used in Pradhan *et al.* (2006) (see Pradhan, 2005 for extensive references). A wide variety of metrics are presented in the literature (Wald *et al.*, 1997; Nunez *et al.*, 1999; Piella and Heijmans, 2003; Ranchin *et al.*, 2003; Shi *et al.*, 2003; Zhou *et al.*, 1998). Many of these different metrics have been inter-compared and found to be redundant (Pradhan *et al.*, 2006). For this study, metrics were selected to minimize redundancy and at the same time show the effect of different metrics. Special attention was given to derive spectral and spatial metrics, as these have opposite trends and should therefore be jointly considered. A brief explanation of these metrics follows.

Spectral Quality Metrics

Inter-band Correlation

Pearson’s correlation coefficient measures the degree of linear relationship between two variables, in this case images. It can vary between -1 to $+1$, indicating complete dissimilarity to perfect analogy of two images. The formula to compute the correlation between two images A and B , both of size $N*N$ pixels, is given by Equation 1:

$$Corr(A | B) = \frac{\sum_{i=1}^N \sum_{j=1}^N (A_{ij} - \bar{A})(B_{ij} - \bar{B})}{\sqrt{\sum_{i=1}^N \sum_{j=1}^N (A_{ij} - \bar{A})^2 \sum_{i=1}^N \sum_{j=1}^N (B_{ij} - \bar{B})^2}} \quad (1)$$

The inter-correlation between each pair of the unsharpened bands and the sharpened bands was computed and compared, where ideally a zero change in the correlation values would be desirable. The presented test images consist of three spectral bands each, and therefore result in two sets of three interband correlation coefficients each: Corr B1 and B2, Corr B1 and B3, and Corr B2 and B3, for the original and the fused multispectral image, respectively.

Correlation Between Original and Fused Multispectral Bands

As a measure of the spectral similarity between the multispectral image before and after image fusion, the correlation coefficients between analogous bands of the original and fused images were calculated. In case of the artificially degraded test images, the correlation coefficients were derived between the original, full resolution image and the fusion results.

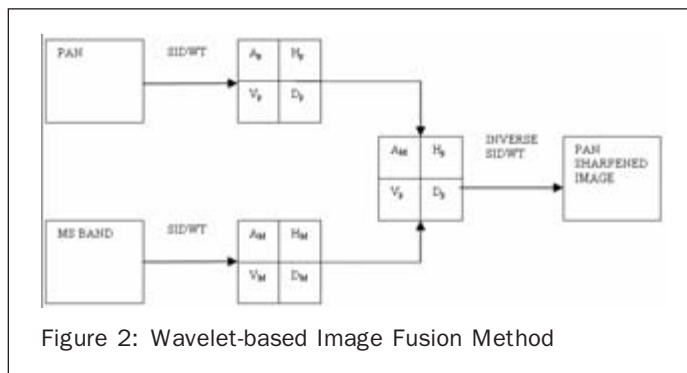


Figure 2: Wavelet-based Image Fusion Method

Root Mean Square Error

The Root Mean Square Error (RMSE) between each unsharpened MS band and the corresponding sharpened band was computed as a further measure of spectral fidelity. This quantifies the average amount of change per pixel due to the processing (i.e., the pan-sharpening) and is described by Equation 2. In this equation, B and F refer to the MS images (resampled to the PAN image size) and the pan-sharpened images, respectively. The subscript k denotes the respective band number in the images:

$$RMSE_k = \frac{\sum_{i=1}^N \sum_{j=1}^N \sqrt{(B_k(i, j) - F_k(i, j))^2}}{N^2} \quad (2)$$

As described in Pradhan *et al.* (2006), it was found that the RMSE is a more sensitive discriminator than Pearson's correlation coefficient. Thus, if the performance of the two image fusion algorithms is almost identical, the RMSE can better distinguish the degree of similarity between original and fused multispectral bands than can the correlation coefficient.

Spatial Quality Metrics

Two spatial quality metrics were applied, both based on a comparison of edge information contained in the fused image and the underlying panchromatic image.

Pearson's Correlation Between HP Filtered PAN and Fused Images

The presence and strength of gradients in the fused image can be visually expressed and quantified with HP filters (Zhou *et al.*, 1998). Upon image fusion, the spatial gradients contained in the fused image should resemble those of the underlying high resolution panchromatic image. The correlation coefficient between HP filtered images of the fused bands and the panchromatic band, respectively, will therefore illustrate the degree of similarity of their spatial gradients. In this study, correlation coefficients were derived for images filtered with a 9*9 pixel HP kernel, both for the average image of the three fused bands, and for each band separately.

RMSE of Sobel Filtered Fused and Panchromatic Bands

As a second spatial metric, the RMSE was derived for edge images, generated with the Sobel edge operator, of the sharpened and panchromatic bands. The Sobel operator consists of a horizontal and a vertical gradient operator and detects edges with a 3*3 filter matrix. The overall gradient image is derived as the Euclidean sum of the resulting two edge images, i.e., the horizontal and the vertical. The RMSE was calculated between the gradient image of the panchromatic band and that of the single fused bands, as well as between the gradient image of the panchromatic band and that of the average image of the fused bands.

Results

In this section, the fusion results based on the HPFA and wavelet techniques are shown, together with the metrics derived for comparison.

Test Case 1: Landsat-7, Denver, Colorado

As shown in Plate 3, the overall visual impression of the HPFA and wavelet-based results is quite similar. Sharpness, colors, and structures are comparable. Slight differences can be found with regard to small water areas, which are rendered somewhat brighter by the wavelet-based fusion. The latter can also be seen to be somewhat "noisier" (more

strongly textured) in homogeneous areas (e.g., agricultural areas) than the HPFA result.

These subtle differences are also reflected in the metrics (Table 2), which derive from a larger image area than the image chip shown. The largest differences are shown by the two RMSE metrics, especially by the Sobel RMSE which reflects textural differences. Here the wavelet-based result has a larger deviation from the PAN image than does the HPFA result.

Test Case 2: Landsat-7, Vorarlberg, Austria

In case of the Landsat image from Vorarlberg, there are more obvious visual differences between the HPFA and the wavelet-based fusion results. These are seen in the two images in Plate 4c and 4d. Again, overall sharpness, color, and structure of the merged Landsat images are similar. However, the wavelet-based fusion introduces relatively strong edge effects. These show strongly as bright edges on the sides of water bodies in the upper left quarter of the image, and as dark lines along the inner edges of water bodies in the right half of the image. The HPFA-1 fusion result shows these effects to a lesser extent.

Plate 4e shows the same Landsat ETM+ multispectral data merged with IRS PAN data (seen in Plate 4f). This image fusion sample was included to illustrate the influence of the different PAN image, with higher spatial resolution (5.8 m), different grey tones and different edges (due to a different acquisition date), on the fusion result.

Compared with the metrics of the wavelet-based fusion result, HPFA-1 shows a significantly higher spectral fidelity with regard to the original multispectral image, but at the same time, the Edge Correlation and Sobel metrics are inferior to the wavelet-based result (Table 3).

Test Case 3: Airphoto, MSU Campus, Mississippi

The image fusion pair shown in Plate 1g, 1h, and 1i illustrates a resolution ratio of 4 (the airphoto was degraded by a factor of 4). Again, the HPFA result and the wavelet-based result are quite similar, with only minimal differences in color tone, structure, and texture. One deviating detail is that the wavelet-based fusion introduces an edge effect on the roof in the upper left quarter of the image, rendering the elongated blue structure on this roof (trending SSW to NNE) somewhat broader than in the original image. Both fusion results provide a close reproduction of the original image.

The metrics (Table 4) quantify these slight differences. Spectrally, the HPFA result has somewhat better values, and the edge correlation is higher than that of the wavelet-based result. The Sobel RMSE, on the other hand, reflects a greater textural similarity between the wavelet-based result and the (simulated) "PAN" image than with the HPFA fusion result. As before, the metrics presented in the table refer to a larger image than the image chips shown in the plate.

Discussion

The HPFA-based fusion is fine-tuned by means of three parameters: high-pass filter size, center value of filter kernel, and injection weight of the added high-pass filtered image. These parameters depend in particular on the ground resolution ratio of the merged images, but also on each other. For example, a larger resolution ratio necessitates a larger high-pass filter kernel size and a higher injection weight. It may also necessitate two-pass processing, which adds additional high frequency detail. The HPFA method, as the fusion samples in this report show, preserves the original spectral properties of the multispectral imagery to a high degree. A larger resolution ratio and injection weight results in a greater change in the original

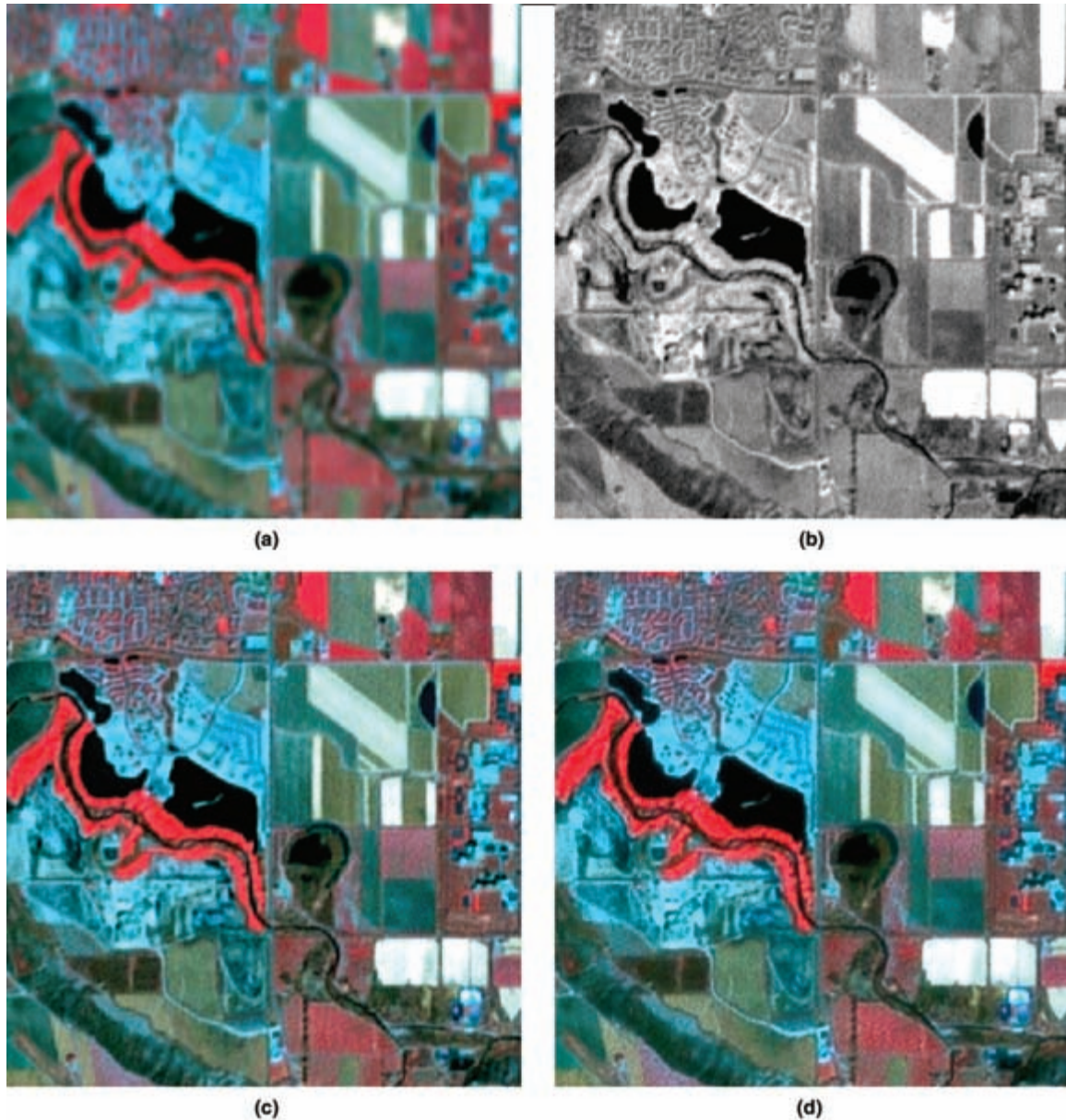


Plate 3: Original Imagery and Fusion Results: Denver, Landsat-7: (a) Landsat-7 EMT+, Bands 2,3,4, (b) Landsat-7, Panchromatic Band, (c) HPFA Fusion Result, and (d) Wavelet-based Fusion Result.

spectral properties. Nevertheless, the colors are not generally distorted by higher resolution ratio fusions: they merely appear somewhat less saturated (see Plate 4e with a resolution ratio of 5.2). It has been shown that a two-pass fusion technique (using two HP filter kernel sizes) is a valuable approach to cope with larger resolution ratios (>5) between the input images.

A visual comparison of the resulting images shows a close similarity between the HPFA and the wavelet-based fusion results in terms of sharpness and spectral properties. Both methods tend to introduce some false edges along existing image edges that have a contrast reversal between the multispectral and the panchromatic images. In the case of Landsat ETM+, this occurs most obviously at water edges in the visible bands. In test case 2, this effect is stronger in the wavelet-based fusion results than in the HPFA fusion

results. With the HPFA method, this effect can be reduced by decreasing the contrast between water and other areas in the PAN image prior to deriving the HPF image, and by slightly increasing the center value of the high-pass filter kernel.

The spectral metrics, in general, indicate a somewhat better preservation of the spectral image properties when using HPFA. The spatial metrics are somewhat ambivalent and show mixed results; sometimes the HPFA results and sometimes the wavelet-based results rank higher. In this context, it should be not overlooked that wavelet-based image fusion itself is a multi-faceted domain with numerous possible implementations. The wavelet-based fusion technique used in this study is based on an extensive testing of that approach (Pradhan, 2005). This underscores the good performance of the HPFA fusion in comparison to

TABLE 2. METRICS FOR LANDSAT ETM+ IMAGE (BANDS 2,3,4), DENVER; RESOLUTION RATIO 2

Fusion Results	Inter-band Correlation Coefficient 1-2, 1-3, 2-3 of pan sharpened MS	Correlation Coefficient of MS and pan sharpened MS analogue bands			RMSE of MS and pan sharpened MS			Edge (HP9) Correlation Coefficient	Edge (Sobel) RMSE
	MS: 0.969, 0.601, 0.596	2	Band 3	4	2	Band 3	4	3 Band Mean and Single Bands	3 Band Mean and Single Bands
HPFA	0.971, 0.644, 0.638	0.980, 0.980, 0.980			1.47, 2.81, 2.96			0.954 0.903, 0.905, 0.929	2.33 5.61, 4.65, 3.93
Wavelet	0.971, 0.633, 0.628	0.976, 0.979, 0.980			1.63, 3.06, 3.16			0.956 0.896, 0.907, 0.938	3.42 6.33, 5.26, 4.55

wavelet-based image fusion. A less rigorous wavelet approach would rank even lower.

For large area image fusion, or mosaics, several further considerations must be taken into account. The injection weight of the HPF image depends on the global standard deviation of each multispectral band. When image mosaics are the intended product, image fusion should be performed *after* mosaicking. Cloud and snow areas, as well as other extreme brightness differences within images, tend to raise the overall standard deviation to a level where injection weights of the HPF image become either generally too high (rendering the fusion results overly crisp with negative spectral and spatial impacts) or too high for parts of the image with a lower regional or local standard deviation. This calls for a further standardization of the method that accounts for these regional differences of the SD in the multispectral images. For example, it can be proposed to work with areas of interest (AOI) and thereby exclude certain areas from the calculation of the SD or separately process different image regions. However, based on numerous tests and applications, including large areas, the HPFA fusion method works satisfyingly over whole satellite scenes which are free of these “extreme” SD differences.

Some preliminary experiments have been performed on HPFA-based fusion of optical and radar imagery. Plate 2b shows an image fusion example where Landsat (bands 1, 2, 3) and RADARSAT (standard beam, 12.5 m pixels) images have been merged. These images of the Mississippi River (seen meandering NW to SE) were acquired during a period of flood produced by high rainfall and seasonal melt. Deep, still water is black due to specular reflection. Some flooded areas are light or dark grey. This may be the result of water surface micro-relief (due to winds or currents) or may be caused by radar scattering from partially covered vegetation. Note that roads and field edges are clearly elucidated in flooded areas and that flooded fields are easily separated from non-flooded.

When much of the area is cloud-covered during an inundation, as in this example, radar and especially synoptic radar – optical merge images are preferable for rescue operations. Post-flood, such images are useful to validate insurance claims.

Another application of radar-optical merges is the improvement of the apparent ground resolution of moderate resolution optical imagery, such as MODIS or MERIS. A fusion test was performed with simulated 300 m optical data and ASAR (30 m) radar data. It showed that the appropriate image scale of the 300 m optical data, which is about 1:1000000, could be improved up to a factor of four (as determined visually) when merged with 30 m ASAR data using the HPFA technique. Topographic and man-made features are highlighted in the merged imagery, due to the injection of radar structures, and make this product valuable for image interpretation.

Conclusion and Outlook

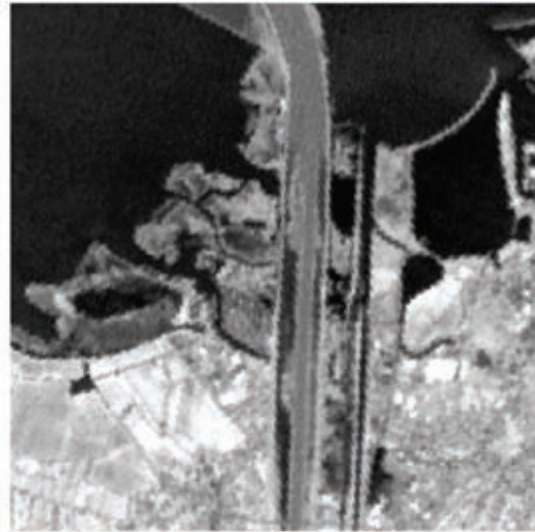
This paper presents an updated version of the high-pass additive method for image fusion, earlier proposed by Chavez *et al.* (1991). This method falls into the spatial domain of image fusion techniques. These techniques preserve the original multispectral properties of the input images to a high degree. The HPFA fusion method has not received much attention in the literature and was considered inferior to other techniques in the spatial domain. One of the novel approaches of this research was that results from the HPFA fusion method were compared with results from a related, but far more researched and accepted technique, wavelet-based image fusion. Three test cases are presented, two use Landsat imagery (resolution ratio 2), and one is a fusion example using a degraded airphoto (resolution ratio 4). The fusion results were compared visually, as well as by means of spectral and spatial metrics. The use of both categories of metrics is important as they tend to show

TABLE 3: METRICS FOR LANDSAT ETM+ IMAGE (BANDS 1,2,3), VORARLBERG; RESOLUTION RATIO 2

Fusion Results	Inter-band Correlation Coefficient 1-2, 1-3, 2-3 of pan sharpened MS	Correlation Coefficient of MS and pan sharpened MS analogue bands			RMSE of MS and pan sharpened MS			Edge (HP9) Correlation Coefficient	Edge (Sobel) RMSE
	MS: 0.938, 0.779, 0.877	2	Band 3	4	2	Band 3	4	3 Band Mean and Single Bands	3 Band Mean and Single Bands
HPFA	0.942, 0.795, 0.886	0.968, 0.968, 0.968			2.08, 1.96, 2.53			0.719 0.704, 0.738, 0.698	17.75 17.10, 16.72, 18.54
Wavelet	0.947, 0.794, 0.881	0.929, 0.929, 0.956			3.18, 3.04, 2.95			0.811 0.896, 0.907, 0.938	16.76 16.44, 16.87, 16.05



(a)



(b)



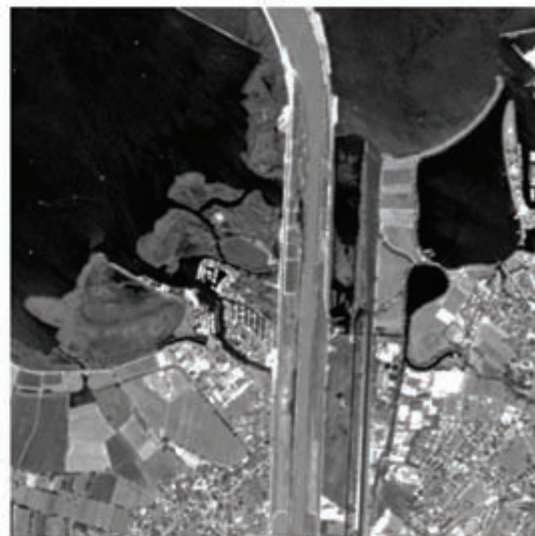
(c)



(d)



(e)



(f)

Plate 4: Original Imagery and Fusion Results: Vorarlberg, Austria: (a) Landsat-7 EMT+, Bands 1,2,3, (b) Landsat Panchromatic Band, (c) HPFA Fusion Result 1, Landsat MS/PAN, (d) Wavelet-based Fusion Result, Landsat MS/PAN, (e) HPFA Fusion Result 2, Landsat MS/IRS PAN (Copyright EurlImage), and (f) IRS PAN. All color images are depicted with the same look-up table.

TABLE 4. METRICS FOR AERIAL PHOTOGRAPH OF MSU CAMPUS; RESOLUTION RATIO 4

Fusion Results	Inter-band Correlation Coefficient 1-2, 1-3, 2-3 of pan sharpened MS	Correlation Coefficient of MS and pan sharpened MS analogue bands			RMSE of MS and pan sharpened MS			Edge (HP9) Correlation Coefficient	Edge (Sobel) RMSE
	Full resolution MS: 0.958, 0.928, 0.969	1	2	3	1	2	3	3 Band Mean and Single Bands	3 Band Mean and Single Bands
HPFA	0.965, 0.944, 0.984	0.993, 0.989, 0.982			3.28, 3.72, 5.39			0.943	8.49
Wavelet	0.969, 0.944, 0.978	0.989, 0.987, 0.984			4.91, 4.50, 5.70			0.916, 0.949, 0.946 0.926	9.73, 13.83, 13.75 6.52
								0.926, 0.921, 0.904	5.04, 10.03, 10.94

opposite trends, reflecting the trade-off between spatial and spectral quality of the fusion results.

The HPFA method, in its conventional application, is considered to have two major deficiencies: the box filter having little frequency selection and the absence of an injection model. For large resolution ratios of the image pairs (5 and higher), the relatively low frequency of the required large filter kernels (e.g., a 11*11 pixel HP filter for a resolution ratio of 5) was indeed found to insufficiently extract the finer spatial details of the PAN imagery. At the same time, the inferior or lacking injection model of the conventional HPFA method often leads to a strong reduction of the color saturation of the merged images or to unusable results. These two major deficiencies of the conventional HPFA fusion can be overcome by the presented refinement of the method. This optimized HPFA method can be applied in a largely standardized way over a wide range of resolution ratios between the input multispectral and panchromatic (or structure/texture providing) images. The use of a second, smaller box filter for large resolution ratios results in refined high frequency details in addition to the overall sharpening effect of the larger HP filter kernel. Importantly, the injection weight for adding the HP image to the multispectral bands is determined automatically. It can be adjusted so as to prioritize either a high spectral fidelity or produce a highly crisp fusion result, compromising spectral quality. Modifying the HP filter center value, finally, is another tuning function for improving spatial structures, though also (somewhat) at the expense of color saturation.

Deficiencies in the modified HPFA method result mainly from the fact that the injection model, though significantly improved, is based on global image parameters. These vary among images and also, when applied to smaller image parts, between these parts. Consequently the injection weight of the HP information varies accordingly between different images, and may be distorted by extremely bright features such as clouds and snow, which result in very heterogeneous radiometric image properties. Water areas, on the other hand, are usually very homogeneous, and may therefore be too strongly sharpened. The introduction of "false edges", frequently along water banks, is another effect of local over-sharpening, but results also from contrast differences and contrast reversals between the PAN and the multispectral images. These false edges can also be observed in wavelet based fusion results.

As quantified with spectral and spatial metrics, as well as based on visual comparison, the redundant wavelet-based fusion technique and the HPFA method deliver quite similar results and perform equally well overall. In addition, preliminary tests of the HPFA method with radar-optical merges showed promising results.

The HPFA technique resulting from this study has been implemented into ERDAS Imagine[®] software and is available with Version 9.0. Future research issues of interest are a regional refinement of the HP injection to better cope with large variations of regional image properties (e.g., snowcover, clouds), segment-based image classification approaches applied to merged imagery (including higher resolution ratio merges), and the further development and testing of the fusion of hybrid images, such as optical and radar.

Acknowledgments

The authors would like to thank Leica Geosystems for providing resources to this work and the means for publishing the color plates, as well as GeoVille for contributing test imagery. Moreover, we are grateful for the suggestions of the reviewers that helped improve this paper.

References

- Aiazzi, B., L. Alparone, S. Baronti, and A. Garzelli, 2002. Context-driven fusion of high spatial and spectral resolution data based on oversampled multiresolution analysis, *IEEE Transactions on Geoscience and Remote Sensing*, 40(9):2300-2312.
- Aiazzi, B., L. Alparone, S. Baronti, I. Pippi, and M. Selva, 2003. Generalised Laplacian pyramid-based fusion of MS + P image data with spectral distortion minimisation, URL: <http://www.isprs.org/commission3/proceedings02/papers/paper083.pdf> (last date accessed: 10 May 2008).
- Burrus C.S., R.A. Gopinath, and H. Guo, 1998. *Introduction to Wavelets and Wavelet Transforms - A Primer*, Prentice Hall, New Jersey, 282 p.
- Carter, D.B., 1998. *Analysis of Multiresolution Data Fusion Techniques* Master Thesis Virginia Polytechnic Institute and State University, URL: <http://scholar.lib.vt.edu/theses/available/etd-32198-21323/unrestricted/Etd.pdf> (last date accessed: 10 May 2008).
- Castleman K.R., 1996. *Digital Image Processing*, Prentice Hall, New Jersey, 667 p.
- Chavez, P.S., S.C. Sides, and J.A. Anderson, 1991. Comparison of three different methods to merge multiresolution and multispectral data: Landsat TM and SPOT panchromatic, *Photogrammetric Engineering & Remote Sensing*, 57(3):295-303.
- Ehlers, M., 2005. Beyond pansharpening: Advances in data fusion for very high resolution remote sensing data, URL: <http://www.ipi.uni-hannover.de/html/publikationen/2005/workshop/127-ehlers.pdf> (last date accessed: 10 May 2008).
- Garzelli, A., 2002. Wavelet-based fusion of optical and SAR image data over urban area, *Proceedings of the ISPRS Technical Commission III Symposium - Photogrammetric Computer Vision (PCV'02)* 09-13 September, Graz, Austria, URL: <http://www.isprs.org/commission3/proceedings02/papers/paper054.pdf> (last date accessed: 10 May 2008)

- González-Audicana, M., L.S. Jose, R.G. Catalan, and R. Garcia, 2004. Fusion of multispectral and panchromatic images using improved IHS and PCA mergers based on wavelet decomposition, *IEEE Transactions on Geoscience and Remote Sensing*, 42(6):1291–1299.
- King, R., and J. Wang, 2001. A wavelet-based algorithm for pan sharpening Landsat 7 imagery. *Proceedings of the International Geoscience and Remote Sensing Symposium*, 2:849–851.
- Lemeshewsky, G. P., 2002. Multispectral image sharpening using a shift-invariant wavelet transform and adaptive processing of multiresolution edges, *Visual Information Processing XI* (Z. Rahman and R.A. Schowengerdt, editors), Proceedings of SPIE, pp. 4736.
- Mallat, S., 1989. A theory for multiresolution signal decomposition: The wavelet representation, *IEEE Transactions on Pattern Analysis and Machine Intelligence*, 11(7):674–693.
- Mercer, J.B., D. Edwards, J. Maduck, G. Hong, and Y. Zhang, 2005. Fusion of high resolution radar and low resolution multi-spectral optical imagery, *Proceedings of the IEEE International Geoscience and Remote Sensing Symposium, IGARSS'05*, 25-29 July, Seoul, South Korea, URL: http://www.intermap.com/images/papers/IGARSS_2005_Mercer.pdf (last date accessed: 10 May 2008).
- Nunez, J., X. Otazu, O. Fors, A. Prades, V. Pala, and R. Arbiol, 1999. Multiresolution-based image fusion with additive wavelet decomposition, *IEEE Transactions on Geoscience and Remote Sensing*, 37(3): 1204–1211.
- Piella, G., and H. Heijmans, 2003. A new quality metrics for image fusion, *Proceedings of International Conference on Image Processing*, Vol. 3, pp. 173–176.
- Pohl, C., and J.L. Van Genderen, 1998. Multisensor image fusion in remote sensing: Concepts, methods and applications, *International Journal of Remote Sensing*, 19(5):823–854.
- Pradhan, P., R. King, N.H. Younan, and D.W. Holcomb, 2006. The effect of decomposition levels in wavelet-based fusion for multi-resolution and multi-sensor images, *IEEE Transactions on Geoscience and Remote Sensing*, 44(12):3674–3686.
- Pradhan, P., 2005. *Multiresolution Based, Multisensor, Multispectral Image Fusion*, Ph.D. dissertation, Mississippi State University, Mississippi State, 208 pages.
- Ranchin, T., B. Aiazzi, L. Alparone, S. Baronti, and L. Wald, 2003. Image fusion – ARSIS concept and some successful implementation schemes, *ISPRS Journal of Photogrammetry and Remote Sensing*, Vol. 58, pp. 4–18.
- Schowengerdt, R.A. 1980. Reconstruction of multispatial, multispectral image data using spatial frequency content, *Photogrammetric Engineering & Remote Sensing*, 46(10):1325–1334.
- Shi, R., C. Zhu, and X. Yang, 2003. Multi-band wavelet for fusing SPOT panchromatic and multispectral images, *Photogrammetric Engineering & Remote Sensing*, 69(5):513–520.
- Steinnocher, K., 1999. Adaptive fusion of multisource raster data applying filter techniques, *International Archives of Photogrammetry and Remote Sensing*, Valladolid, Spain, Vol. 32, Part 7-4-3.
- Strang, G., and T. Nguyen, 1996. *Wavelets and Filter Banks*, Wellesley-Cambridge Press, Wellesley, Massachusetts.
- Wald, L., T. Ranchin, and M. Mangolini, 1997. Fusion of satellite images of different spatial resolutions: Assessing the quality of resulting images, *Photogrammetric Engineering & Remote Sensing*, 63(6):691–699.
- Yocky, D.A., 1995. Image merging and data fusion by means of the two-dimensional wavelet transform, *Journal of the Optical Society of America*, 12(9):1834–1845.
- Zhang, Y., 1999. A new merging method and its spectral and spatial effects, *International Journal of Remote Sensing*, 20(10):2003–2014.
- Zhang, Y., 2002. Problems in the fusion of commercial high-resolution satellite images as well as Landsat 7 images and initial solutions, *International Archives of Photogrammetry and Remote Sensing*, Vol. 34, Part 4: GeoSpatial Theory, Processing and Applications, Ottawa, URL: <http://www.isprs.org/commission4/proceedings02/pdfpapers/220.pdf> (last date accessed: 10 May 2008).
- Zhou J., D.L. Civco, and J.A. Silander, 1998. A wavelet transform method to merge Landsat TM and SPOT panchromatic data, *International Journal of Remote Sensing*, 19(4):743–757.

(Received 28 August 2006; accepted 03 November 2006; revised 12 January 2007)